Eur. Phys. J. B **10**, 555–562 (1999)

THE EUROPEAN PHYSICAL JOURNAL B

EDP Sciences

Tetragonal structure of thin nickel films on Cu(001)

P. Le Fèvre[1,a], H. Magnan[1,2], and D. Chandesris[1]

[1] Laboratoire pour l'Utilisation du Rayonnement Électromagnétique, Université Paris-Sud, Bâtiment 209d, B.P. 34, 91898 Orsay Cedex, France
[2] Commissariat à l'Énergie Atomique, Service de Recherche sur les Surfaces et l'Irradiation de la Matière, 91191 Gif-sur-Yvette Cedex, France

Received 22 December 1998

Abstract. The crystallographic structure of thin Ni films deposited on Cu(001) has been studied using Surface Extended X-ray Absorption Fine Structure (SEXAFS). Taking advantage of the linear polarization of the synchrotron radiation, we have shown that Ni adopts the Cu lattice parameter parallel to the interface. This lateral expansion induces a longitudinal compression of the unit cell, leading to a face centered tetragonal structure of the Ni films from 3 to 10 monolayers. The temperature dependence of the EXAFS oscillations has allowed to measure strain inside the Ni layers.

PACS. 68.55.-a Thin film structure and morphology – 75.70.Ak Magnetic properties of monolayers and thin films – 68.35.Ja Surface and interface dynamics and vibrations

1 Introduction

Thin films deposited on single-crystal substrates have been the subject of numerous studies during the last decade. It appeared that one could stabilize original crystallographic phases for a large range of elements, thus creating a new class of materials. Their bidimensional character, together with the occurrence of singular crystallographic structures, often confer to these thin films electronic properties that can not be found in bulk solids.

For magnetic transition metals layers, the appearance of magnetization easy axis perpendicular to the film plane (Perpendicular Magnetic Anisotropy: PMA) is a typical bidimensional effect. It has been observed in various systems, *e.g.* Fe/Ag(001) [1], Fe/Cu(001) [2], Co/Pt(111) [3] or Co/Au(111) [4]. In these cases, PMA is mainly due to the truncated environment of the surface atoms (Néel anisotropy), an effect whose influence decreases as compared to bulk effects, when the thickness of the film increases. Thus, in all the systems quoted above, a PMA was observed only up to a critical thickness, always of the order of some monolayers (ML). In the Fe/Cu(001) system, it was also shown that PMA exists only in Fe films with a disordered and distorted structure [5].

A link between macroscopic quantities (like magnetic anisotropy constants) and microscopic observations (lattice distortion, local disorder, growth mode...) is quite delicate to find [6]. Obviously, a clear explanation of the magnetic properties of thin films, as well as improvements of theoretical models, require a precise characterization of the film crystallography, with all the available experimental techniques.

It is particularly true for the Ni/Cu(001) system, considered in this paper: magnetic measurements have shown that, for Ni layers thinner than 7 ML, the magnetization easy axis lies in the film plane, but switches perpendicular to the film plane for larger thicknesses [7,8]. PMA is observed up to 60 Å for Ni/Cu/Si(001) [9], up to 110 Å in Cu/Ni/Cu(001) sandwiches [10], and up to 140 Å in Cu/Ni/Cu/Si(001) [11,12]. It is the epitaxial system which exhibits a perpendicular magnetization in the largest thickness range. This magnetic anisotropy, very different from those previously observed, can not be ascribe to a surface contribution. Three specific properties of this system can help to understand the origin of this remarkable behaviour. First, magnetostatic effects (which drive the magnetization in the film plane at large thicknesses) are relatively small in Ni. Second, thanks to a reasonable lattice mismatch, one can stabilize coherent epitaxial thin Ni layers on a Cu substrate. Last, the Ni large magnetoelastic coupling coefficient implies large effects of the epitaxial strains on the PMA [9]. All the models proposed to explain the thickness dependent magnetic easy axis of the Ni/Cu(001) films have introduced a bulk [7,10,12] (and surface [9,11]) magnetoelastic term, induced by a tetragonal structure of the Ni films. This structure should result from the adaptation of the Ni lattice to the Cu one. Ni and Cu are both fcc metals, with lattice parameters of, respectively, 3.52 Å and 3.61 Å. Ni is supposed to adopt the Cu lattice parameter parallel to the interface up to a given thickness, varying from 10 [13]

[a] e-mail: plefevre@lure.u-psud.fr

to 18 Å [9]. This lateral expansion of the cell should induce a longitudinal contraction (elastic deformation), thus leading to a tetragonal structure of Ni on Cu(001).

This tetragonal structure has been qualitatively observed by photoelectron diffraction [14], and a first characterization by quantitative Low Energy Electron Diffraction (LEED) has been published recently [13]. The purpose of this paper is to present a Surface Extended X-Ray Absorption Fine Structure (SEXAFS) study of Ni thin films on Cu(001).

The differences between SEXAFS and LEED measurements for the study of thin films are well known. First, X-ray absorption is element selective: by recording a spectrum at the Ni K-edge, we are only sensitive to the environment of the Ni atoms, without any contribution of the substrate [15]. Second, it is a strength of the quantitative LEED technique to give informations about the very first interlayer distances in the sample, but it is nearly blind to the deeper atomic planes. SEXAFS provides first nearest neighbour (FNN) distances and widths of radial distribution functions (RDF) averaged on the whole film. Third, using the linear polarization of the synchrotron radiation (used as photon source), SEXAFS allows to measure lattice parameters in all the crystallographic directions with the same accuracy, in a quite direct way [5,16,17]. LEED is a well suited technique to extract interlayer distances (including possible relaxations), but it is difficult to obtain precise quantitative crystallographic informations parallel to the interface. Furthermore, analysis of quantitative LEED data requires sophisticated programs and numerous fitting parameters. In this paper, fits of the SEXAFS data are done with a maximum of two free parameters. Recent theoretical developments allow now a complete calculation of X-ray absorption spectra, in the multiple scattering formalism [18]. Simulations of experimental data give access to informations which were available in the spectra but not reachable by the classical EXAFS analysis methods, in the single scattering formalism [16,17]. In the present case, multiple scattering calculations will allow a precise and quantitative determination of the tetragonal structure of the Ni films, by an analysis of the distant neighbours shells contributions to the EXAFS signal. Finally, the temperature dependence of the XAFS data will allow to describe the strain in the Ni films [19].

After a description of the experimental details in Section 2, we will present the results on structure and strain in Sections 3 and 4.

2 Experimental details

The experiments were carried out at the Laboratoire pour l'Utilisation du Rayonnement Électromagnétique (LURE, France), on the wiggler beam line of the DCI storage ring, using a Ge(220) double crystal monochromator, at the Ni K-edge (8 333 eV). The Cu(001) single crystal substrate was cleaned by Ar^+ ionic bombardments at 870 K. The cleanliness and the good crystallographic quality of the Cu surface were checked respectively by Auger spectroscopy and LEED. Ni was deposited at room temperature from a high purity wire heated by electronic bombardment, in a vacuum better than 3×10^{-10} mbar. Deposition rates were calibrated prior to the evaporation with a quartz microbalance; thicknesses were controlled by Auger spectroscopy and by measuring the absorption edge jump. The SEXAFS measurements were done *in situ* at room temperature and at 77 K, in the total yield mode.

3 Tetragonal structure of Ni on Cu(001)

The oscillations of the X-ray absorption coefficient (EXAFS oscillations) are due to perturbations to the absorption of an isolated atom by his surrounding neighbours. These oscillations are therefore directly correlated to the structure and the local order around the excited atom. A Fourier transform (FT) of the EXAFS oscillations gives a series of peaks corresponding to the different shells of neighbours of the excited atom [20]. An inverse Fourier transform (IFT) of the first peak of the FT allows to isolate the contribution of the FNN shell from the total signal. This contribution χ_1 can be fitted using a simple formula

$$\chi_1(k) = \frac{N_1^*}{kR_1^2} A(k) \mathrm{e}^{-2k^2\sigma^2} \sin\left[2kR_1 + \varphi(k)\right] \qquad (1)$$

χ_1 is given as a function of k, the wave vector of the photoelectron created in the absorption process, which is related to the photon energy $h\nu$ by

$$h\nu - E_\mathrm{l} = \frac{\hbar^2 k^2}{2m}$$

where E_l is the binding energy of the core level. $A(k)$ (Ni backscattering amplitude) and $\varphi(k)$ (phase shift) are electronic parameters. In our case, they were easily determined from a bulk Ni reference EXAFS spectrum. The electron mean free path is taken into account in the $A(k)$ function. Knowing these electronic parameters, one can extract the crystallographic parameters (R_1, σ^2 and N_1^*) by fitting the experimental data with formula (1). R_1 is the FNN distance, and σ^2 is the mean square relative displacement, giving the width of the radial distribution function. σ^2 contains two contributions: the thermal agitation (Debye-Waller factor) and the static disorder. The values of σ^2 obtained with the fits is the difference between the mean square relative displacement in the sample and in the reference. N_1^* is an apparent number of FNN, given by

$$N_1^* = 3 \sum_{j=1}^{N_1} \cos^2 \alpha_j \qquad (2)$$

where α_j is the angle between the polarization of the X-ray and the bond between a Ni atom and his jth FNN.

From this formula, it appears that the EXAFS oscillations depend on the polarization direction of the X-rays with respect to the sample crystallographic structure: the contribution of each bond to the total signal is weighted

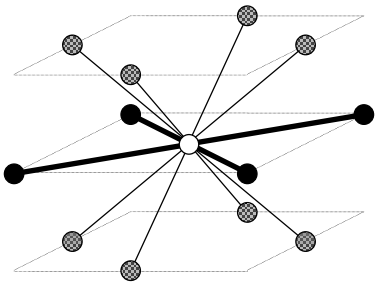

Fig. 1. First nearest neighbour shell of a Ni atom (open circle) in a face centered tetragonal structure. Each Ni atom has four first nearest neighbours in the same (001) plane (in-plane bonds) (closed circles), and eight out of this plane (out-of- plane bonds) (cross hatched circles). For a face centered tetragonal structure, the in-plane bonds are longer than the out-of-plane ones. Despite these two different distances, the twelve atoms surrounding a given Ni atom will be simply called the first nearest neighbour shell in the text.

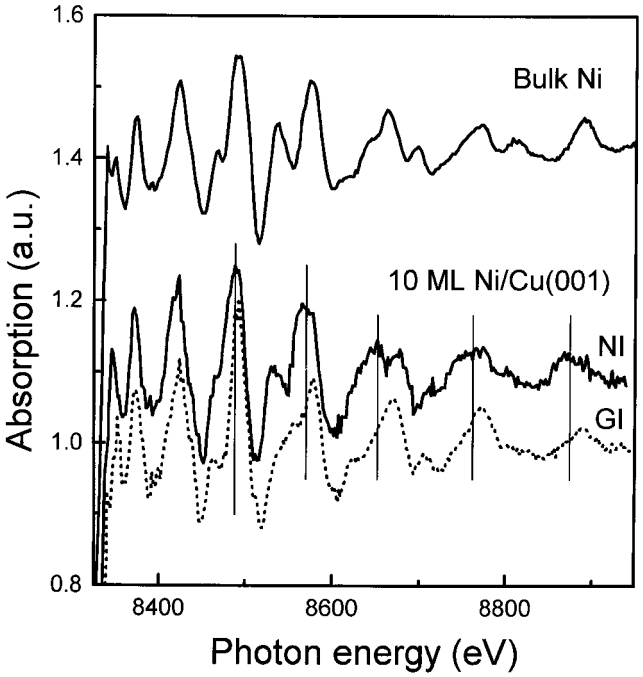

Fig. 2. EXAFS spectra recorded at 77 K on a reference bulk Ni foil (top) and on a 10 ML Ni/Cu(001) film, in normal and in grazing incidence (bottom).

by a the cosine to the square of the angle between the bond and the polarization of the light. Thus, the weight of a precise type of bond can be enhanced or canceled, by changing the angle between the incident X-rays and the crystallographic axis of the sample. We have used the linear polarization of the synchrotron radiation to measure a possible distortion of the Ni lattice. In the following analysis, we have supposed a homogeneous structure in the whole Ni film. For each sample, we have recorded two spectra, with the X-rays coming in normal incidence (NI) (polarization of the X-rays parallel to the surface plane) or in grazing incidence (GI) (polarization of the X-rays almost perpendicular to the surface plane). The FNN shell of a Ni atom is represented in Figure 1, for the supposed tetragonal structure of the thin films. Each Ni atom has twelve FNN, four in the same (001) plane, four above (missing for the top layer), and four below (Cu atoms for the interface Ni layer). Using formula (2), a simple calculation gives that, for the FNN shell, only the eight bonds out of the (001) planes (out-of-plane bonds) contribute to the signal in GI with an apparent weight of twelve, whereas in NI, the four bonds contained in the (001) planes (in-plane bonds) and the eight out of plane bonds contribute with the same apparent weight of 6.

For the supposed tetragonally distorted fcc structure of the Ni films, the in-plane FNN bonds are expected to be longer than the out-of-plane ones. Despite these two different distances, the twelve atoms surrounding a given Ni atom will be simply called the first nearest neighbour shell. The main contribution to the EXAFS signal is due to this FNN shell. As can be seen in formula (1), the FNN distance appears as the main frequency of the oscillations. Thus, the GI EXAFS spectrum main frequency is related to the out-of-plane FNN distance. In the NI spectrum the main frequency is the average of the in-plane and the out-of-plane FNN distances. The raw EXAFS spectra recorded in the two incidences on a 10 ML Ni/Cu(001) sample are presented in Figure 2, together with the spectrum obtained on bulk fcc Ni. First, the general shape of

Table 1. Apparent first nearest neighbours numbers $N^*_{\text{in-plane}}$ and $N^*_{\text{out-of-plane}}$ calculated using formula (2) for all the studied Ni thicknesses, assuming a layer by layer growth mode and a perfect cubic structure.

	3 ML		5 ML		7 ML		10 ML	
	NI	GI	NI	GI	NI	GI	NI	GI
$N^*_{\text{in-plane}}$	6	0	6	0	6	0	6	0
$N^*_{\text{out-of-plane}}$	5	10	5.4	10.8	5.6	11.14	5.7	11.4

the EXAFS oscillations are different in the thin film and in fcc Ni. It is particularly clear in the structures around 8 570 and 8 650 eV. This indicates that Ni is not fcc in the thin films. Second, the NI spectrum oscillates with a higher frequency than the GI spectrum. As explained above, it shows that in-plane FNN distances are larger than the out-of-plane ones.

More quantitatively, the out-of-plane FNN bond length ($R_{\text{out-of-plane}}$) and its associated mean square relative displacement ($\sigma_{\text{out-of-plane}}$) can be measured by fitting the experimental contribution in GI of the FNN shell ($\chi_1^{\text{GI}}(k)$) with formula (1):

$$\chi_1^{\text{GI}}(k) = \frac{N^*_{\text{out-of-plane}}}{kR^2_{\text{out-of-plane}}} A(k) \mathrm{e}^{-2k^2\sigma^2_{\text{out-of-plane}}} \times \sin\left[2kR_{\text{out-of-plane}} + \varphi(k)\right].$$

Knowing this out-of-plane bond length, one can deduce the in-plane FNN bond length ($R_{\text{in-plane}}$) and its associated mean square relative displacement ($\sigma_{\text{in-plane}}$) by fitting the FNN shell contribution extracted from the NI

Table 2. FNN distances determined by a least-squares fits of the experimental data using formula (1), for the spectra recorded at 300 K and 77 K, in normal and in grazing incidence, on Ni/Cu(001) thin films for different Ni thicknesses. $R_{\text{in-plane}}$ (respectively $R_{\text{out-of-plane}}$) is the length of the first nearest neighbour bonds contained in the (001) planes (respectively out of these planes).

	3 ML		5 ML		7 ML		10 ML	
	RT	77 K	RT	77 K	RT	77 K	RT	77 K
$R_{\text{in-plane}}$ (Å)	2.55 ± 0.01	2.54 ± 0.01	2.54 ± 0.01	2.55 ± 0.01	2.55 ± 0.01	2.55 ± 0.01	2.55 ± 0.01	2.55 ± 0.01
$R_{\text{out-of-plane}}$ (Å)	2.51 ± 0.01	2.51 ± 0.01	2.50 ± 0.01	2.50 ± 0.01	2.50 ± 0.01	2.51 ± 0.01	2.50 ± 0.01	2.50 ± 0.01

spectrum ($\chi_1^{\text{NI}}(k)$) using

$$\chi_1^{\text{NI}}(k) = \frac{A(k)}{k}\left[\frac{N^*_{\text{out-of-plane}}}{R^2_{\text{out-of-plane}}} e^{-2k^2\sigma^2_{\text{out-of-plane}}} \times \sin\left[2kR_{\text{out-of-plane}} + \varphi(k)\right] + \frac{N^*_{\text{in-plane}}}{R^2_{\text{in-plane}}} \times e^{-2k^2\sigma^2_{\text{in-plane}}} \sin\left[2kR_{\text{in-plane}} + \varphi(k)\right]\right].$$

In the fits, the N^* were fixed to their theoretical values for a layer by layer growth mode. These values are listed in Table 1. The FNN distances obtained from the fits are presented in Table 2. For all the studied Ni thicknesses, we obtain a $R_{\text{in-plane}}$ of 2.55 ± 0.01 Å, a value equal to the FNN distance in the Cu substrate (2.55 Å). $R_{\text{out-of-plane}}$ remains also constant with Ni thickness, with a value of 2.50 ± 0.01 Å. These in-plane and out-of-plane FNN distances show directly that, from 3 to 10 ML, the Ni films are in a face centered tetragonal structure, with lattice parameters parallel to the interface $a_{\parallel} = 3.61 \pm 0.02$ Å, and perpendicular to the interface $a_{\perp} = 3.46 \pm 0.04$ Å. Such a structure has already been observed in thin cobalt films deposited on Cu(001) [16].

This tetragonal structure can be confirmed by observing the polarization dependence of the distant neighbours shells contributions to the EXAFS signal. The FT of the EXAFS spectra recorded on the 3 ML and the 10 ML Ni films in NI and in GI are plotted in Figure 3. The main peak is due to the FNN shell, the peaks located at higher R being due to the more distant neighbours shells. In NI, we see three well defined peaks around 3.3, 4 and 4.7 Å (labelled A, B and C in Fig. 3), while in GI these peaks shift to respectively 2.9, 3.9 and 4.5 Å. Is this polarization dependence due to the tetragonal structure of the films? As a matter of fact, since the structure is distorted, the EXAFS spectra are different in NI and in GI (see Fig. 1): the $\langle 001 \rangle$ directions are no longer equivalent as in a cubic structure. This must give a clear polarization dependence of the distant peaks of the FT.

In order to confirm the tetragonal structure of the Ni films, we have performed complete simulations of the polarization dependent X-ray absorption spectra, starting from a Ni cluster built with the lattice parameters deduced from the FNN shell analysis. This was done using the FEFF6 code, which calculates the absorption cross-section in a multiple scattering formalism [17]. It was

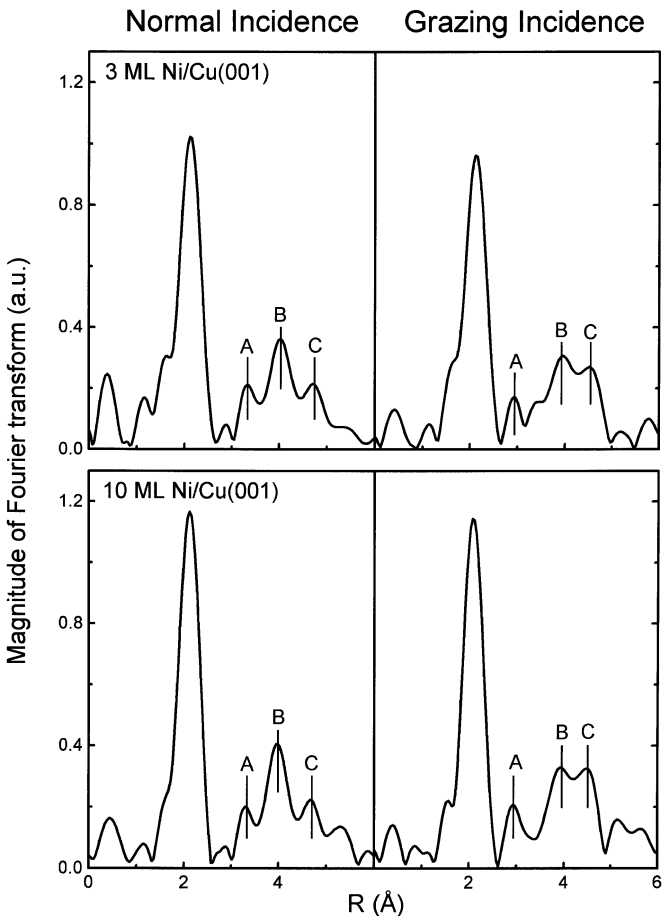

Fig. 3. Fourier transforms (calculated from $k = 2.55$ Å^{-1} to $k = 12.35$ Å^{-1}) of the EXAFS spectra recorded on a 3 ML Ni/Cu(001) film (top) and on a 10 ML Ni/Cu(001) film (bottom), in normal (left) and in grazing (right) incidence.

shown that this code provides very good results on $3d$ transition metals [16,17,21]. The FT of the experimental spectra recorded on the 10 ML Ni/Cu(001) film are compared in Figure 4 to calculations done on a tetragonal Ni cluster. The best agreement was achieved with lattice parameters of $a_{\parallel} = 3.61$ Å and $a_{\perp} = 3.42$ Å, very close to those determined by the FNN shell analysis. Both the NI and the GI spectra are well described in this model. Moreover, the positions of the peaks are very sensitive to slight variations of the lattice parameters, as it was shown on thin cobalt films on Cu(001), where the same

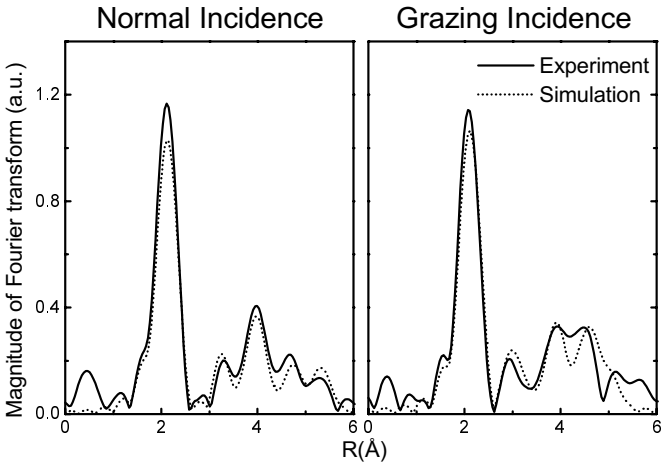

Fig. 4. Comparison between Fourier transforms (calculated from $k = 2.55$ Å^{-1} to $k = 12.35$ Å^{-1}) of experimental EXAFS spectra recorded on a 10 ML Ni/Cu(001) film (solid line), and simulations calculated by the FEFF6 code for tetragonal Ni, with lattice parameters $a_{\parallel} = 3.61$ Å and $a_{\perp} = 3.42$ Å (dotted line) ($R_{\text{in-plane}} = 2.55$ Å and $R_{\text{out-of-plane}} = 2.49$ Å), in normal (left) and in grazing (right) incidence. For the calculations, we used a Debye temperature of 450 K, and a S_0^2 of 1.

tetragonal structure, with identical lattice parameters, was evidenced [16]. The agreement between experiments and simulations therefore confirms the tetragonal structure of the Ni films, and the crystallographic parameters extracted from the FNN shell analysis.

In the previously quoted study of Co films on Cu(001) [15], the Co tetragonal structure was explained by an elastic deformation of a cubic cell, using the continuum elastic theory. In this approach, $a_{\perp}$ and $a_{\parallel}$ should be linked by the formula

$$\frac{\Delta a_{\perp}}{a_{\perp}} = -2\frac{C_{12}}{C_{11}}\frac{\Delta a_{\parallel}}{a_{\parallel}}$$

where C_{11} and C_{12} are the standard elastic coefficients in a cubic crystal. $a_{\parallel}$ was found to be imposed by the Cu substrate (3.61 Å), and, using $C_{12}/C_{11} = 0.578$ [22], one obtains $a_{\perp} = 3.42$ Å. This leads to out-of-plane FNN distances of 2.49 Å, a value very close to the one determined by the SEXAFS measurements.

Despite a quite large lattice mismatch (2.6%), the Ni tetragonal structure can be considered as an elastic deformation of the bulk cubic Ni cell, and is well described by the continuum elastic theory as previously observed for thin Co films deposited on the same Cu(001) substrate [16]. Our results clearly demonstrate a tetragonal structure for Ni in the whole film volume, for all the thicknesses up to 10 ML. This is the first experimental evidence of this distortion which was the basis of most of the magnetic models. According to reference [6], the magnetoelastic energy can be simply written as

$$E_{\text{ME}} = VB\varepsilon \sin^2\theta$$

where V is the volume of the Ni film, B is a magnetoelastic constant, ε the strain in the Ni film, and θ the angle between the film normal and the magnetization. Assuming a constant strain in a given range of thicknesses, the magnetoelastic energy, which favors a PMA in this system, is here proportional to the film thickness. It is only in this case that, above a critical thickness, this magnetoelastic energy can compensate the surface anisotropy, which favors an in-plane magnetization [7,13]. In different approaches [6,9,11], above a critical thickness t_{c}, strain relaxations have been introduced. The film growth is therefore no more coherent with the Cu substrate. The strain ε is then often given by

$$\varepsilon \sim -\eta\frac{t_{\text{c}}}{t}\,.$$

This leads to a magnetoelastic energy which does no longer depend on the film thickness. One can account only in this regime for the switch of the magnetization easy axis from perpendicular to in-plane. Our experimental evidence of absence of relaxation up to 10 ML is therefore crucial for the validation of magnetic models, and a possible prediction of the switching thickness.

4 Elastic properties of the Ni films

As pointed out above, the mean square relative displacement σ^2 arising in the EXAFS formula contains two contributions, thermal agitation (Debye-Waller factor) and the static disorder. σ^2 depends therefore on temperature T, and can be written

$$\sigma^2(T) = \sigma^2_{\text{DW}}(T) + \sigma^2_{\text{stat}}.$$

A comparison between EXAFS spectra recorded at 300 K and at 77 K allows to measure the amplitude of thermal vibrations. First, the contributions of the FNN shell, χ_1 (77 K) and χ_1 (300 K), are extracted from the experimental spectra. Assuming that the structural parameters and the static disorder do not change with temperature, the ratio between these contributions is

$$\frac{\chi_1\ (300\ \text{K})}{\chi_1\ (77\ \text{K})} = \mathrm{e}^{-2k^2\left(\sigma^2_{\text{DW}}(300\ \text{K})-\sigma^2_{\text{DW}}(77\ \text{K})\right)} = \mathrm{e}^{-2k^2\Delta\sigma^2_{\text{DW}}}.$$

A plot of the logarithm of the ratio $\frac{\chi_1\ (300\ \text{K})}{\chi_1\ (77\ \text{K})}$ as a function of k^2 gives a straight line with a slope of $2\Delta\sigma^2_{\text{DW}}$, where $\Delta\sigma^2_{\text{DW}}$ is the difference between the relative mean square displacements (due to phonons) at 300 and 77 K [19]. This analysis done on the NI and the GI spectra allows to determine a $\Delta\sigma^2_{\text{DW-NI}}$ and a $\Delta\sigma^2_{\text{DW-GI}}$. The EXAFS Debye-Waller factor is only sensitive to relative motions of a FNN with respect to the central atom. It is therefore different from the mean square displacement, measured, *e.g.*, by diffraction experiments. An example of the determination of $\Delta\sigma^2_{\text{DW-NI}}$ and $\Delta\sigma^2_{\text{DW-GI}}$ on the 7 ML Ni film is presented in Figure 5. As pointed out before, the GI spectra contain only contributions from the out-of-plane bonds. The $\Delta\sigma^2_{\text{DW-GI}}$ therefore directly measure the thermal motion

Table 3. Differences of the mean square relative displacement due to thermal agitation between 300 K and 77 K, extracted from the GI ($\Delta\sigma^2_{\text{DW-GI}}$) and NI ($\Delta\sigma^2_{\text{DW-NI}}$) EXAFS spectra. Using simple models (see text), one can deduce mean square relative displacements for FNN bonds in the (001) planes ($\Delta\sigma^2_{\text{DW-in-plane}}$) and out of these planes ($\Delta\sigma^2_{\text{DW-out-of-plane}}$), as well as parallel ($\Delta\sigma^2_{\parallel}$) and perpendicular ($\Delta\sigma^2_{\perp}$) to the interface. Einstein frequencies ($\omega_{\parallel}$ and $\omega_{\perp}$) are associated to these latest values; the ratio of the force constants are derived from these vibrations frequencies.

	3 ML	5 ML	7 ML	10 ML
$\Delta\sigma^2_{\text{DW-NI}}$ ($\times 10^{-3}$ Å^2)	4.4 ± 0.3	4.4 ± 0.3	4.2 ± 0.3	3.1 ± 0.3
$\Delta\sigma^2_{\text{DW-GI}}$ ($\times 10^{-3}$ Å^2)	3.2 ± 0.3	3.7 ± 0.3	3.4 ± 0.3	3.1 ± 0.3
$\Delta\sigma^2_{\text{DW-in-plane}}$ ($\times 10^{-3}$ Å^2)	5.6 ± 0.3	5.1 ± 0.3	4.8 ± 0.3	3.1 ± 0.3
$\Delta\sigma^2_{\text{DW-out-of-plane}}$ ($\times 10^{-3}$ Å^2)	3.2 ± 0.3	3.7 ± 0.3	3.4 ± 0.3	3.1 ± 0.3
$\Delta\sigma^2_{\parallel}$ ($\times 10^{-3}$ Å^2)	5.6 ± 0.3	5.1 ± 0.3	4.8 ± 0.3	3.1 ± 0.3
$\Delta\sigma^2_{\perp}$ ($\times 10^{-3}$ Å^2)	1.5 ± 0.3	2.8 ± 0.3	2.6 ± 0.3	3.1 ± 0.3
$\omega_{\parallel}$ ($\times 10^{13}$ Hz)	3.1 ± 0.1	3.2 ± 0.1	3.3 ± 0.1	3.9 ± 0.1
$\omega_{\perp}$ ($\times 10^{13}$ Hz)	5.2 ± 0.1	4.0 ± 0.1	4.2 ± 0.1	3.9 ± 0.1
$\frac{\kappa_{\parallel}}{\kappa_{\perp}}$	$0.3 \pm 30\%$	$0.6 \pm 30\%$	$0.6 \pm 30\%$	$1.0 \pm 30\%$

along this bonds, $\Delta\sigma^2_{\text{DW-out-of-plane}}$. In NI, the problem is more complex, since each spectrum contain the contributions of two types (in-plane and out-of-plane) of bonds. Nevertheless, using the cumulants development [23] for two types of bonds having close lengths and neglecting a k^4 term, one can show that the logarithm of the amplitude ratio is $2\Delta\sigma^2_{\text{DW-NI}}$, where

$$\Delta\sigma^2_{\text{DW-NI}} = \frac{\Delta\sigma^2_{\text{in-plane}} + \Delta\sigma^2_{\text{out-of-plane}}}{2}$$

$\Delta\sigma^2_{\text{DW-in-plane}}$ measuring the thermal motion along the in-plane bonds. The complete results obtained for Ni thicknesses from 3 to 10 ML are compiled in Table 3. In principle, one must obtain the same values by calculating the differences between the σ^2 determined in the fits of the FNN shell contribution, but this method is more precise, since it does not require any reference spectrum. Assuming a continuous variation of the amplitude of the thermal vibrations between the different crystallographic directions (see Fig. 6), one can calculate the mean square relative displacements parallel ($\Delta\sigma^2_{\parallel}$) and perpendicular ($\Delta\sigma^2_{\perp}$) to the interface.

Except for the 10 ML film, $\Delta\sigma^2_{\parallel}$ is always larger than $\Delta\sigma^2_{\perp}$. It indicates intralayer force constant between Ni atoms weaker than the interlayer one up to 7 ML. This trend was already observed by high resolution Electron Energy Loss Spectroscopy (EELS) on 1 and 2 ML samples [24,25]. It is not that surprizing, since a larger interatomic distance should soften the bond, while shorter bonds should stiffen it. For the thinner films, this effect overcomes the surface effect which softens the interlayer bonds [19, 26]. The anisotropic elastic behaviour of the Ni layers is similar to the one observed in thin Co films deposited on Cu(001), but, in this latest case, the elastic constants were still non isotropic up to 15 ML of Co [16].

On the contrary, for the 10 ML Ni film, our measurements, which give an average value on the whole film, show isotropic vibration amplitudes, with a value almost equal to the one measured in bulk Ni (3.2×10^{-3} Å^{-2}; for bulk Cu, we measured a $\Delta\sigma^2$ of 4.7×10^{-3} Å^{-2}), although the structure is still distorted. It is interesting to note that this change in the elastic properties of the Ni film occurs around the thickness where the film magnetization easy axis switches from in-plane to perpendicular to the film plane. Of course, this change alone can not explain this different magnetic behaviour, but it can indicate a different morphology of the Ni film (increase of defaults density, appearance or coalescence of islands...). The observations by Scanning Tunneling Microscopy of large islands in this thickness region could be a clue [27]. The cause of these different elastic properties must be identified, in order to improve the models describing the magnetic properties of the Ni films.

Let us try now to extract from the experimental data a quantitative comparison between force constants perpendicular and parallel to the interface. Sevillano *et al.* proposed a correlated Einstein model, where the correlated phonons density of states is replaced by a $\delta(\omega_{\text{E}})$ function [28]. In this model, the $\Delta\sigma^2_{\text{DW}}$ measured between $T_1 = 300$ K and $T_2 = 77$ K has a simple expression

$$\Delta\sigma^2_{\text{DW}} = \frac{\hbar}{M\omega_{\text{E}}}\left[\coth\left(\frac{\hbar\omega_{\text{E}}}{2k_{\text{B}}T_1}\right) - \coth\left(\frac{\hbar\omega_{\text{E}}}{2k_{\text{B}}T_2}\right)\right]$$

where M is the mass of a Ni atom. Using this expression, one can determined an Einstein frequency ω_{E} for each measured $\Delta\sigma^2_{\text{DW}}$ (see Tab. 3). The force constant κ associated to this Einstein frequency is proportional to ω^2_{E}. Applied to bulk Ni, this crude model gives, within

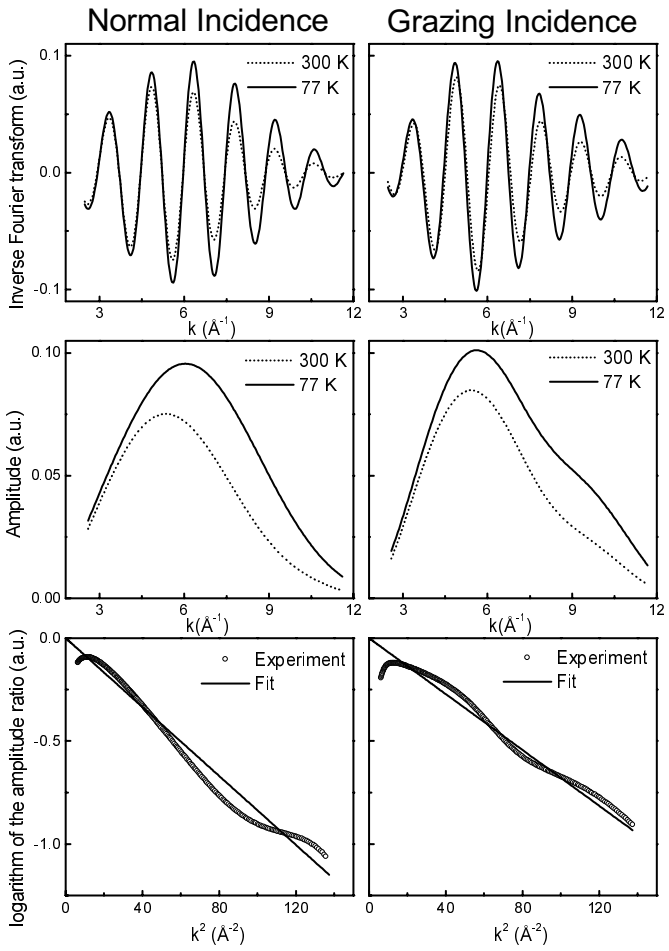

Fig. 5. An example of the determination of $\Delta\sigma^2_{\text{DW-NI}}$ and $\Delta\sigma^2_{\text{DW-GI}}$ on the 7 ML Ni/Cu(001) film. The contributions of the first nearest neighbours shell are isolated from the total EXAFS signal by calculating the inverse Fourier transform of the first peak of the Fourier transform (top), both at 300 K (dotted line) and at 77 K (solid line). The amplitude of these contributions are calculated (middle). The logarithm of the amplitudes ratio as a function of k^2 can be fitted by a straight line with a slope of $\Delta\sigma^2_{\text{DW}}$ (bottom). This analysis done both for spectra recorded in normal incidence (left) and in grazing incidence (right) allows to determine respectively $\Delta\sigma^2_{\text{DW-NI}}$ and $\Delta\sigma^2_{\text{DW-GI}}$.

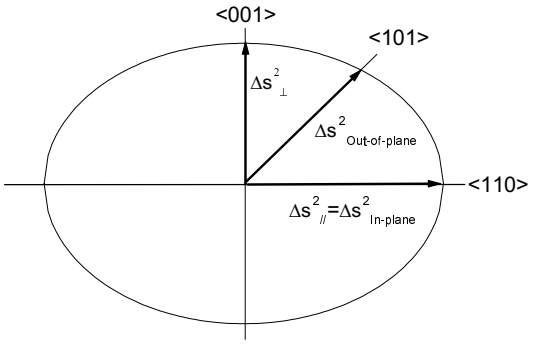

Fig. 6. The simple picture used to describe the atomic vibrations parallel and perpendicular to the interface.

30%, the force constant obtained by more sophisticated methods [29]. We can therefore expect a correct order of magnitude for the ratios between the force constants parallel ($\kappa_{\parallel}$) and perpendicular ($\kappa_{\perp}$) to the interface, calculated respectively from $\Delta\sigma^2_{\parallel}$ and $\Delta\sigma^2_{\perp}$. The calculated values are given in Table 3. Within the error bars, from 3 to 7 ML, the force constant parallel to the interface is two times smaller than the force constant perpendicular to the interface, and about 1.5 time smaller than in bulk Ni. As pointed out before, the thickest studied film (10 ML) shows isotropic force constants, almost equal to the bulk Ni one.

5 Conclusion

The crystallographic structure of thin Ni films deposited on Cu(001) has been studied by Surface EXAFS. Taking advantage of the linear polarization of the synchrotron radiation, we have precisely measured the lattice distortion induced in the films by the epitaxy on the copper single crystal substrate. We have shown that Ni adopts the Cu lattice parameter parallel to the interface; this lateral expansion induces a longitudinal compression of the unit cell. This leads to a face centered tetragonal structure of the Ni films from 3 to 10 monolayers, with lattice parameters parallel to the interface $a_{\parallel} = 3.61 \pm 0.02$ Å, and perpendicular to the interface $a_{\perp} = 3.46 \pm 0.04$ Å. This was confirmed by multiple scattering calculations of the absorption spectra. An identical structure has already been observed in thin cobalt films deposited on Cu(001) [16]. The temperature dependence of the EXAFS oscillations has allowed to measure the elastic properties inside the Ni layers. For thicknesses between 3 to 7 ML, in a simplified approach, we found a force constant parallel to the interface two times smaller than the force constant perpendicular to the interface. A 10 ML film has the same elastic properties than bulk Ni, despite a still distorted structure. This could indicate a changing in the film morphology, corresponding roughly to the switching of the magnetization easy axis. Our study shows that, up to 10 ML, the whole Ni film has a homogeneous tetragonal structure. It therefore justifies the model proposed for the explanation of the magnetic properties of the Ni layers, which assumes a magnetoelastic contribution proportional to the film volume to promote the PMA observed in these films.

We would like to thank M.C. Desjonquères, C. Barreteau and D. Spanjaard for fruitful discussions on theoretical problems concerning the elastic properties of the Ni films.

References

1. B. Heinrich, K.B. Urquhart, A.S. Arrot, J.F. Cochran, K. Myrtle, S.T. Purcell, Phys. Rev. Lett. **59**, 1756 (1987); N.C. Koon, B.T. Jonker, F.A. Volkening, J.J. Krebs, G.A. Prinz, Phys. Rev. Lett. **59**, 2463 (1987); J. Araya-Pochet, C.A. Ballentine, J.L. Erskine, Phys. Rev. B **38**, 7846 (1988).

2. D. Pescia, M. Stampanoni, G.L. Bona, A. Vaterlaus, R.F. Willis, F. Meier, Phys. Rev. Lett. **58**, 2126 (1987); C. Liu, E.R. Moog, S.D. Bader, Phys. Rev. Lett. **60**, 2422 (1988).
3. R. Allensbach, J. Magn. Magn. Mater. **129**, 160 (1994); J. Thiele, C. Boeglin, K. Hricovini, F. Chevrier, Phys. Rev. B **53**, 11934 (1996).
4. R. Allenspach, M. Stampanoni, A. Bischof, Phys. Rev. Lett. **65**, 3344 (1990).
5. H. Magnan, D. Chandesris, B. Villette, O. Heckmann, J. Lecante, Phys. Rev. Lett. **67**, 859 (1991).
6. P. Bruno, J.P. Renard, Appl. Phys. A **49**, 499 (1989); P. Bruno, Phys. Rev. B **39**, 865 (1989).
7. B. Schulz, K. Baberschke, Phys. Rev. B **50**, 13467 (1994); B. Schulz, R. Schartzwald, K. Baberschke, Surf. Sci. **307-309**, 1102 (1994).
8. F. Huang, M.T. Kief, G.J. Mankey, R.F. Willis, Phys. Rev. B **49**, 3962 (1994).
9. G. Bochi, C.A. Ballentine, H.E. Inglefield, C.V. Thompson, R.C. O'Handley, H. Hug, B. Stiefel, A. Moser, H.-J. Güntherodt, Phys. Rev. B **52**, 7311 (1995).
10. R. Jungblut, M.T. Johnson, J. aan de Stegge, A. Reinders, F.J.A. den Broeder, J. Appl. Phys. **75**, 6424 (1994).
11. G. Bochi, C.A. Ballentine, H.E. Inglefield, C.V. Thomson, R.C. O'Handley, Phys. Rev. B **53**, 1729 (1996).
12. R. Naik, C. Kota, J.S. Payson, G.L. Dunifer, Phys. Rev. B **48**, 1008 (1993).
13. S. Müller, B. Schulz, G. Kostka, M. Farle, K. Heinz, K. Baberschke, Surf. Sci. **364**, 235 (1996).
14. Y. Idzerda, G.A. Prinz, Surf. Sci. **284**, L394 (1996).
15. P.A. Lee, Phys. Rev. B **13**, 5261 (1976).
16. O. Heckmann, H. Magnan, P. Le Fèvre, D. Chandesris, J.J. Rehr, Surf. Sci. **312**, 62 (1994).
17. P. Le Fèvre, H. Magnan, O. Heckmann, V. Briois, D. Chandesris, Phys. Rev. B **52**, 11462 (1995).
18. J.J. Rehr, J. Mustre de Leon, S.I. Zabinski, R.C. Albers, J. Am. Chem. Soc. **113**, 5135 (1991); J. Mustre de Leon, J.J. Rehr, S.I. Zabinski, R.C. Albers, Phys. Rev. B **44**, 4146 (1991); J.J. Rehr, R.C. Albers, S.I. Zabinski, Phys. Rev. Lett. **69**, 3397 (1992).
19. P. Roubin, D. Chandesris, G. Rossi, J. Lecante, M.C. Desjonquères, G. Tréglia, Phys. Rev. Lett. **56**, 1272 (1986).
20. D.E. Sayers, E.A. Stern, F.W. Lytle, Phys. Rev. Lett. **27**, 1204 (1971).
21. P. Le Fèvre, H. Magnan, D. Chandesris, Surf. Sci. **352-354**, 923 (1996).
22. Simmons and Wang, *Single crystal elastic constants and calculated aggregated properties* (Cambridge Massachusetts, MITpress, 1971).
23. E.D. Crozier, J.J. Rehr, R. Ingalls, in *X-ray Absorption. Principles, Applications, Techniques of EXAFS, SEXAFS and XANES*, edited by D.C. Köningsberger, R. Prins (New York, 1988), Chap. 9.
24. C. Stuhlmann, H. Ibach, Surf. Sci. **219**, 117 (1989).
25. J. Ellis, E.M. McCash, W. Allison, J. Electron. Spectrosc. Relat. Phenom. **54-55**, 325 (1990).
26. P. Roubin, D. Chandesris, G. Rossi, J. Lecante, J. Phys. F **18**, 1165 (1988).
27. J. Shen, J. Giergiel, J. Kirschner, Phys. Rev. B **52**, 8454 (1995).
28. E. Sevillano, H. Meuth, J.J. Rehr, Phys. Rev. B **20**, 4908 (1979).
29. G. Tréglia, M.C. Desjonquères, J. Phys. France **46**, 987 (1985).